Frequency Agility Radar with Overlapping Pulses and Sparse Reconstruction

Jabran Akhtar and Karl Erik Olsen
Norwegian Defence Research Establishment (FFI)
Box 25, 2027 Kjeller, Norway
Email: jabran.akhtar@ffi.no, karl-erik.olsen@ffi.no

***Abstract*— The use of frequency agility has a proven track record in radar systems. Altering the radar carrier frequency over shorter intervals improves the detection capabilities for slowly fluctuating targets and increases jamming resistance. This article exploits the frequency diversity concept further and proposes a transmission structure for emission of pulses overlapping in time. This is combined with the relative more modern framework of compressed sensing and sparse reconstruction for coherent regeneration of signals. Through detailed simulations the performance of such a setup is evaluated. It is shown that the overall system performance can be improved and definitive estimates for target velocities can be obtained even with a sizable reduction in integration time.**

Keywords: Frequency agility, waveform diversity, compressed sensing, sparse reconstruction

I. Introduction

Frequency agility and waveform diversity has long been used in many radar systems as it is a straightforward and simple concept which can significantly improve target detection performance for fading targets. It is an important tool for combating radar jamming and avoiding interference from other sources. In a classical frequency agility system, the radar would interchangeably transmit a pulse, or a number of pulses, on one specific frequency before altering the frequency and transmitting pulses on another carrier frequency. Alternatively, the radar may mainly focus on modifying the waveforms only. Frequent changes in waveforms and frequencies, however, make coherent processing a much more challenging task for the radar as to generate high resolution range-Doppler images numerous identical frequency pulses needs to be transmitted in a single coherent processing interval (CPI) [1]. To save on integration time, standard radar processing with frequency agility may therefore consist of simple incoherent integration of all received data which is feasible with a limited CPI and multiple waveforms; albeit available Doppler information is then not taken full advantage of [2].

The last decade has seen establishment of new data acquisition techniques in which data is collected in a sparse manner and computational methods are used to reconstruct and recover full performance signals [3], [4]. The use of such schemes have also been studied significantly in radar settings [5], [6], [7], [8]. This article takes the basic framework of frequency and waveform diversity one step further by linking it with reduced data sensing in frequency and range and a sparse reconstruction method. Interleaving of waveforms is a familiar radar concept, however, in this background we introduce a pulse transmission strategy where different pulses are emit in an overlapping manner with a greater pulse repetition frequency (PRF). The superimposed pulses are readily separated via matched-filtering due to frequency agility. Repeating the process in specific successive manners provides a design where different ranges are alternating covered by different pulses. In a traditional context such a design is generally not desirable as the data is collected across different frequencies and can not be processed coherently. Nevertheless, this can be shown to provide an advantage for the utilization of sparse reconstruction techniques to fill in empty positions and to recover sparse range-Doppler maps preserving full benefits of coherent integration even with an overall shorter CPI. A thorough study on compressed sensing and frequency agility with regard to target reconstruction performance has not been proposed earlier in the literature.

Previous works, particularly [9], [10], considered the use of sparse data collection from different steering directions for an electronically scanning array based radar and demonstrated how sparse reconstruction can be used to recover simple range-Doppler maps. This was made possible under the assumption that the angular sensing regions are independent and there is thus no need for any assimilation of the results. The final products are therefore multiple unrelated range-Doppler maps. This condition no longer remains valid if the radar utilizes frequency or waveform agility techniques while aiming towards the same direction. The end result then needs to be tied together in a satisfactory manner for e.g. target detection purposes.

In summary, the contributions of this paper are

- A transmission structure with frequency agility and overlapping pulses is proposed tailored specifically for sparse reconstruction to reduce the total dwell time
- Evaluation of coherent processing and Doppler extraction for frequency agility based radar with sparse sensing in range and frequency
- An extension of preceding works with emphasis on frequency diversity and joint optimization techniques

In the remainder of the text, the expression frequency agility and/or waveform diversity is used interchangeably to imply that the radar is either altering frequencies and/or waveforms on a regular basis.

DOI til publisert versjon / DOI to published version: 10.1109/RADAR.2018.8378531

II. Radar signal model

We characterize a radar with frequency agility capabilities where within a specific CPI, the antenna remains pointed towards a fixed direction and a total of N number of pulses are sent and echoes received up to a range R. The pulses are assumed split over Q different carrier frequencies and waveforms, $p_1(t), ..., p_Q(t)$. The targets are assumed to be slowly fading following Swerling one or three distributions and thus the radar cross sections and reflectively levels remains constant within the dwell for one given frequency but are otherwise independent across the Q pulses. The reception of the incoming pulses $s(t,u)$ may therefore be specified more precisely as

$$s(t,u) = \sum_n \sigma_{n,l} p_l(t - \Delta_n) e^{j v_{n,u,l}} + w(t) \tag{1}$$

where t is fast-time, u is slow-time and l, $1 \leq l \leq Q$, indicates the waveform with a set carrier frequency. $\sigma_{n,l}$ are the reflectivity levels of incoming echoes while Δ_n is the delay associated with each reflector n and $j = \sqrt{-1}$. $w(t)$ is white Gaussian noise and $e^{j v_{n,u,l}}$ is the frequency dependent Doppler shift which for a constant velocity object is described by

$$v_{n,u,l} = v_{n,u-1,l} + \frac{\theta_n \, 4\pi f_l}{c \, \text{PRF}}, \tag{2}$$

where θ_n is the radial velocity of target n, f_l being the carrier frequency, PRF is the pulse repetition frequency and c is the speed of propagation [2]. The phase shifts in the observed $s(t,u)$ will only show a consistent linear pattern if l, the carrier frequency, is retained, at least across some parts of the dwell.

The radar is expected to sample the incoming data and perform a matched filtering operation with the most recent emit pulse

$$Y(t,u) = p_l^*(-t) * s(t,u) \tag{3}$$

where $*$ prescribes convolution in fast-time. With a discrete fast-time parameter, corresponding to range bin, the collected data can be specified by the matrix

$$\mathbf{Y}(r,u) = Y(r\ \Delta t, u)\ \in \mathbb{C}^{N \times R},\ r = 1, 2, ..., R, \tag{4}$$

given Δt as the time-resolution of the radar.

A. Traditional processing

A simple traditional processing of the available data may consist of incoherent integration of all pulses,

$$\mathbf{y}(r) = \frac{1}{N} \sum_{u=1}^{N} |\mathbf{Y}(r,u)|^2. \tag{5}$$

Alternatively, a range-Doppler map may be generated by executing a Fourier transform over each range bin column

$$\mathbf{D}(r,\omega) = \mathbf{F}\ (\mathbf{w} \circ \mathbf{Y}(r,u)|_r) \quad \in \mathbb{C}^{N \times R}. \tag{6}$$

where $\mathbf{F}$ is the discrete Fourier matrix of size $N \times N$, $\mathbf{F}_{k,l} = \exp(-j2\pi kl/N)$ and $\mathbf{w}\ \in \mathbb{C}^{N \times 1}$ is a tapering function multiplied element-wise, indicated by $\circ$, on columns of $\mathbf{Y}$. Range-Doppler processing is particularly useful for clutter filtering and estimating target velocities and on-following detection may be carried out via thresholding tests or CFAR variants. Nevertheless, with changing frequencies full coherency can not be established with (6) resulting in low integration gain and targets may show considerable spread in Doppler.

From the above the trade-off between diversity and resolution also becomes evident for a traditional radar framework. To obtain high Doppler resolution all the pulses need to be sent with the same frequency but this comes at the expense of loss of diversity gain. At the other extreme, by transmitting different waveforms on a pulse-to-pulse basis the diversity level is maximized at the expense of coherency. For a given CPI, a desirable goal should be to obtain a set diversity level with high Doppler resolution and the smallest possible time-frame. We next propose a scheme with overlapping frequency diverse pulses and sparse reconstruction in an attempt to achieve that.

In order to simplify the presentation, the rest of the paper is concerned with frequency diversity limited to two independent frequencies though the concept may readily be expanded and a thorough study will be presented elsewhere.

B. Sparse overlapping pulse emissions with two waveforms

We consider a radar system with $Q = 2$ available waveforms which operates in several interchanging modes within a dwell:

- Mode A1: transmission of $p_1(t)$ with a fixed PRF to cover the range interval $[0, R]$. A total of P_1 pulses are sent and received.
- Mode A2: transmission of $p_2(t)$ with a fixed PRF to cover the range interval $[0, R]$. A total of P_2 pulses are sent and received.
- Mode B: P_B number of pulses are emit with twice the PRF as of mode A1 or A2 and the waveforms are successively alternated between $p_1(t)$ and $p_2(t)$. The most recent transmitted pulse therefore only covers the range $[0, R_1]$ (near region) while returns still arriving from the past pulse encompass $[R_1, R]$ (far region).

We define T to reflect the time between sending a pulse and receiving back echoes enclosing the full range up to R, and the mid-range is $R_1 = R/2$. A conventional radar system normally operates by alternating modes A1 and A2 only. With the new mode B operating with a higher PRF the pulses will overlap in time but covering different ranges. The receiver therefore performs a matched-filtering with both waveforms on the incoming signals

$$Y_1(t,u) = p_1^*(-t) * s(t,u),\ Y_2(t,u) = p_2^*(-t) * s(t,u). \tag{7}$$

As long as emit pulses are on different frequencies, or otherwise have good cross-correlation properties, the interference will be minimal and the radar can place the sampled matched-filtered data at appropriate positions at the near or far regions in $\mathbf{Y}_1(r,u)$ or $\mathbf{Y}_2(r,u)$. $\mathbf{Y}_1(r,u)$ and $\mathbf{Y}_2(r,u)$ as (4) but pointing to data collected with the respective waveforms, $p_1(t)$ or $p_2(t)$. A possible transmission pattern for mode B is provided in table I where the transmission and reception of each pulse occurs within the shorter time interval of $T/2$. The

Dette er en postprint-versjon / This is a postprint version.
DOI til publisert versjon / DOI to published version: 10.1109/RADAR.2018.8378531

range region covered by each pulse is also indicated at the top.

#	Current, $[0, R_1]$	Previous, $[R_1, R]$	Duration
1	$p_1(t)$	–	T/2
2	$p_2(t)$	$p_1(t)$	T/2
3	$p_1(t)$	$p_2(t)$	T/2
4	$p_2(t)$	$p_1(t)$	T/2
5	$p_1(t)$	$p_2(t)$	T/2
6	$p_2(t)$	$p_1(t)$	T/2
7	–	$p_2(t)$	T/2

TABLE I: Example of mode B sequence

A total of 6 pulses are sent in the example with a higher PRF though the effective PRF for each waveform is still identical to the one of mode A1 or A2. The pulses therefore correspond to the same time-frame as of 3 mode A pulses but the observation time is reduced in half and the arrangement forces a sparse sampling of ranges with alternating frequencies. In practice there will be blind regions around the first range bin and around R_1 when a new pulse is emit though the impact of that is ignored for the time being. More sophisticated transmission patterns may be designed incorporating for example conjugated or negated pulses and randomized pulse selection. We further assume that the last emit pulse is also captured from the far region extending the total duration by $T/2$. Altogether, this example gives raise to a total of 4 range-Doppler map reconstructing problems: two independent range-Doppler maps for the near region with $p_1(t)$ and $p_2(t)$ and similarly two independent range-Doppler maps for the far region with the two different pulses. Any targets in these two range-Doppler maps exhibiting independent fading.

One consequence of the pattern of table I is that for a particular waveform the structure is comparable to having a PRF which is just half of the original PRF. Due to the very regular transmission setup the mutual coherence can be high [11] and this can further lead to ambiguities in Doppler. For firm unambiguous outcomes mode B should ideally be combined with mode A1/A2, either interleaved within the transmission structure or as separate entities before or after mode B. An example of such sequence is given in table II which a total span of $7.5T$. By replenishing empty gaps this should ideally result in the same performance as of 11 full range pulses implying a time saving of over 30%. The example combined block starts with mode A2 and ends with A1.

#	Current, $[0, R_1]$	Previous, $[R_1, R]$	Duration
1	$p_2(t)$	–	T
2	$p_2(t)$	–	T
3	$p_1(t)$	–	T/2
4	$p_2(t)$	$p_1(t)$	T/2
5	$p_1(t)$	$p_2(t)$	T/2
6	$p_2(t)$	$p_1(t)$	T/2
7	$p_1(t)$	$p_2(t)$	T/2
8	$p_2(t)$	$p_1(t)$	T/2
9	–	$p_2(t)$	T/2
10	$p_1(t)$	–	T
11	$p_1(t)$	–	T

TABLE II: Example of mode A and B combined sequence

The total duration for a block with mode A1, A2 and mode B can be determined as

$$T_{tot} = T(P_1 + P_2) + T(P_B + 1)/2. \tag{8}$$

The major purpose of the scheme is therefore be to make certain that even with a shorter time-duration and sparse data collection comparable results can be achieved to if all pulses were sent with a lower PRF and full range coverage.

C. Coupled sparse regeneration

Taking note of the fact the described transmitting and receiving setup is a radar sampling sparsely across different frequency bands and regions one can attempt to reconstruct full-resolution range-Doppler maps for each of the given frequencies. For the technique of this subsection we expand the basic algorithms presented in [9], [10] and refer to them for more detailed characterization. The original methods of the earlier works are designed to fill in empty gaps in collected data and possibly also perform an extrapolation in Doppler domain to obtain higher resolution sparse range-Doppler maps. As the main objective with diverse waveforms is to improve detection capabilities, which is often performed by merging all profiles into a single one, a coupled optimization technique can accordingly be adapted to maximize the joint sparsity for each range bin over all frequencies.

To streamline, we define the following:

- The matrix $\mathbf{Y}_l(r, u)$ only incorporates values reciprocal to pulse/frequency l after matched-filtering with $p_l^*(-t)$
- $\mathbf{y}_l|_r$ refers to a column of $\mathbf{Y}_l(r, u)$ corresponding to range r
- L points to the number of desired output entries in the reconstructed Doppler domain with $L \geq N$, an $L > N$ signifying Doppler domain extrapolation
- The binary selection matrix for frequency l and correspondingly range r, $\mathbf{M}_{l,r} \in \mathbb{B}^{N \times L}$, is generated by taking an $L \times L$ identity matrix $\mathbf{I}_{L \times L}$ and removing the respective rows for which no data is collected
- $\hat{\mathbf{G}}_{l,r} = \mathbf{M}_{l,r}\hat{\mathbf{F}}^* \in \mathbb{C}^{N_l \times L}$ is the partial inverse Fourier matrix of $L \times L$ Fourier matrix $\hat{\mathbf{F}}$
- $\bar{\mathbf{w}}_{l,r} = \mathbf{M}_{l,r}\hat{\mathbf{w}} \in \mathbb{C}^{N_l \times 1}$ is the truncated window function generated from $\hat{\mathbf{w}}$ which is an L point window function
- $||\ ||_1$ indicates L_1 norm
- ε is acceptable error in reconstruction

In the case of two alternating waveforms there will be a set of four reconstructing matrices, occurring from the possible combinations of near or far region and pulse $p_1(t)$ or $p_2(t)$.

Expanding cited papers, the reconstruction problem for the Doppler profiles of a given range r can thus be formulated as

$$\begin{bmatrix} \tilde{\mathbf{D}}_1(r, \hat{\omega})|_r \\ \tilde{\mathbf{D}}_2(r, \hat{\omega})|_r \end{bmatrix} = \arg\min || \begin{bmatrix} \dot{\mathbf{d}}_1 \\ \dot{\mathbf{d}}_2 \end{bmatrix} ||_1 \tag{9}$$

$s.t.$

$$|| \begin{bmatrix} \tilde{\mathbf{G}}_{1,r} & 0 \\ 0 & \tilde{\mathbf{G}}_{2,r} \end{bmatrix} \begin{bmatrix} \dot{\mathbf{d}}_1 \\ \dot{\mathbf{d}}_2 \end{bmatrix} - \begin{bmatrix} \bar{\mathbf{w}}_1 \circ \bar{\mathbf{y}}_1|_r \\ \bar{\mathbf{w}}_2 \circ \bar{\mathbf{y}}_2|_r \end{bmatrix} ||_2 \leq \varepsilon. \tag{10}$$

Dette er en postprint-versjon / This is a postprint version.
DOI til publisert versjon / DOI to published version: 10.1109/RADAR.2018.8378531

Iterating this process over all ranges leads to two different sparsely regenerated range-Doppler maps, $\tilde{\mathbf{D}}_1(r,\hat{\omega})$ and $\tilde{\mathbf{D}}_2(r,\hat{\omega})$ over the two frequencies. The main advantage of a range based optimization is that it does not restrict the overall number of targets in the range-Doppler profile as the sparsity condition only applies to individual range bins where the likelihood of multiple targets present at the exact same range is much smaller. The solutions may be transformed from Doppler domain back to slow-time and combined with real data to regenerate a hybrid range-Doppler plot, $\hat{\mathbf{H}}_l(r,\hat{\omega})$ where only the original empty gap contain reconstructed data while otherwise the real data is retained as is [10]. Finally, under the assumption that the Doppler bins correspond to approximately the same velocities, a combined squared range-Doppler map may be employed for e.g. target detection:

$$\tilde{\mathbf{H}}^2(r,\omega) = \frac{1}{\sqrt{2}}(|\tilde{\mathbf{H}}_1(r,\hat{\omega})|^2 + |\tilde{\mathbf{H}}_2(r,\hat{\omega})|^2) \in \mathbb{C}^{L\times R}. \quad (11)$$

The next section investigates in detail the performance level of the proposed radar architecture.

III. Simulations and Analysis

In order to compare and analyze the performance of the proposed techniques we model a radar system operating at 3.3GHz with a PRF of 2kHz. The frequency of the second waveform is placed 1% apart and for the first simulation cases we assume a single target with a velocity of 25m/s positioned at a range bin corresponding to 1.8km from the radar. The PRF is kept constant while the target reflectively values are assumed to be constant for the duration of the dwell over the same frequency while they are independent across frequencies and randomly picked from Swerling 1 distributions. The mean radar cross section (RCS) of the target is varied to account for various signal-to-noise ratios (SNR). Noise is independently Gaussian distributed with the mean level at -16 dBm. The Blackman window has otherwise been employed throughout. Although uncomplicated, this radar model contains all the essential elements to accurately provide the main results on the aspects of frequency agility with respect to sparse range sampling and reconstruction. The simulations are performed over the transmission structure of table II and we point out that the number of pulses available for integration and reconstruction is thus small to provide for a challenging environment. For the first reconstructions $L = 11 + 8 = 19$ is set which corresponds to total extrapolation of $E = 8$ samples split equally at the beginning and end of the original sequence. E is used to convey the total number of extrapolations in the reconstruction.

A. Illustrative example

This subsection provides an illustrative example on how the proposed scheme can work in practice for a single realization. Two random RCS values are selected for the target giving rise to single pulse SNR of -0.27 dB and 6.19 dB, respectively, over the two frequencies. A standard range-Doppler plot (6) consisting of data as collected through $\mathbf{Y}(r,u) = \sum_{l=1}^{2} \mathbf{Y}_l(r,u)$. is shown in figure 1 while figure 2 presents the result of incoherent integration (5). The value of ε is set as a scaled version of the assumed a priori noise level and the end result from the proposed sparse reconstruction process (11) is shown in figure 3. This image therefore contains real simulated data where available while reconstructed samples are incorporated only at empty gaps and for extrapolation. The scaling of all the plots is respect to the maximum obtained value assimilating all integration and coherency gains.

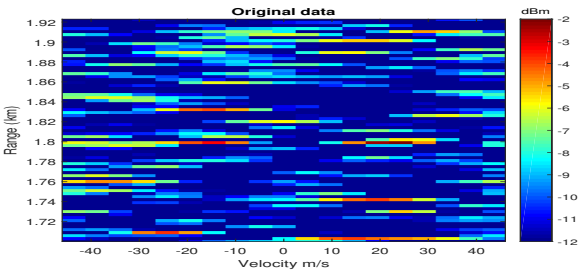

Fig. 1: Standard R-D map

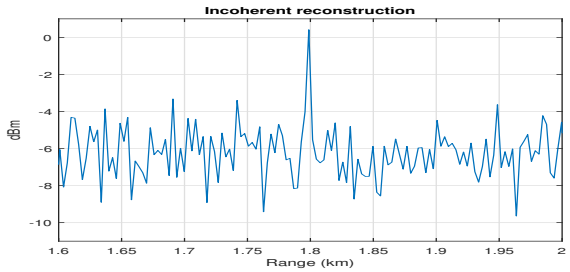

Fig. 2: Incoherent integration

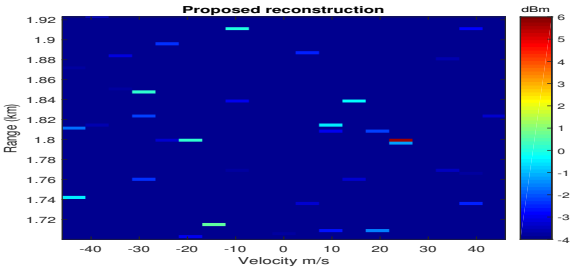

Fig. 3: Hybrid reconstruction, $E = 8$

From the outcomes it is easy to observe that although standard range-Doppler processing does bring forth the target under these SNR levels the obtained integration gain is limited and the spread in Doppler is also very significant with ambiguous velocity. The standard technique has basically not been able to deal with this type of sparse emission and reception structure. Incoherent integration provides a slightly better gain which is still only 4 dB above the noise floor. The sparse reconstructing process leading to the final hybrid image offers a very noticeable 6 dB additional gain and the target appears very clearly localized at a particular Doppler velocity. Since this is a hybrid image presence of spikes arising from the inaccuracies present in the original data set can be recognized.

Dette er en postprint-versjon / This is a postprint version.
DOI til publisert versjon / DOI to published version: 10.1109/RADAR.2018.8378531

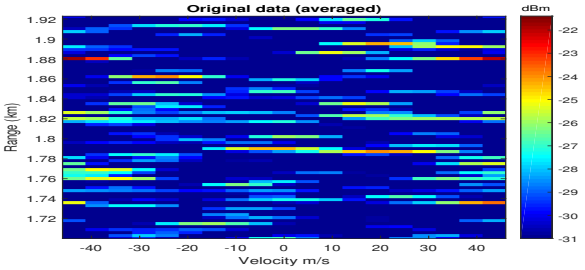

Fig. 4: Standard R-D, mean SNR = 0 dB

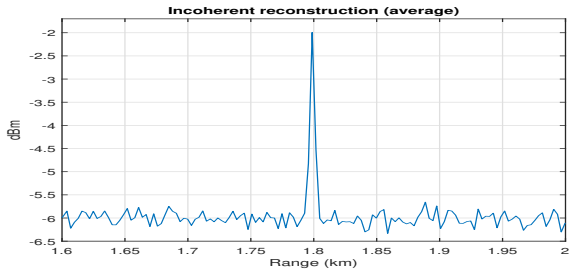

Fig. 5: Incoherent integration, mean SNR = 0 dB

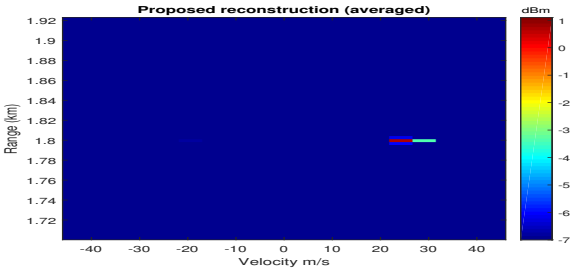

Fig. 6: Hybrid reconstruction, mean SNR = 0 dB, $E = 8$

B. Signal to noise ratio and extrapolation

The single example above demonstrates some important aspects, but for more detailed understanding a statistical framework is required. We next look at the average outcomes coming from a large number of Monte Carlo simulations. A total of 1000 independent simulations, following the previous description, are performed with the target values selected randomly over the two frequencies for each run from a Swerling 1 distribution with a given single pulse SNR. The averaged plots for a mean SNR of 0 dB can be seen in figures 4 to 6. Even though the target is visible in the standard range-Doppler plot it is on par with noisy spikes and difficult to distinguish as a target. Incoherent detection, averaged, performs better while the proposed sparse reconstruction with $E = 8$ extrapolations can easily make the target stand out in a coherent manner. There is a gain improvement of 3 dB in contrast with incoherent processing.

The mean gain levels achieved as a function of single pulse SNR are given in figure 7. For very low SNR levels the incoherent method is marginally better, otherwise the sparse reconstruction method provides a definitive improvement alongside the advantage of being able to estimate Doppler velocity.

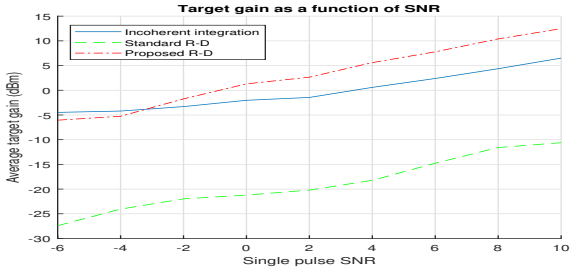

Fig. 7: Mean target gain

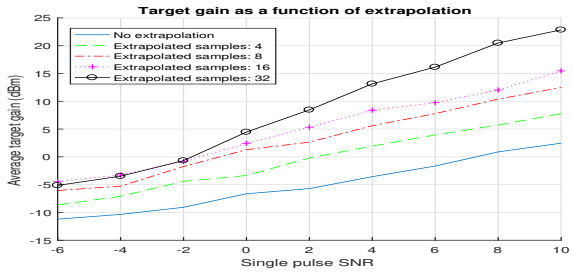

Fig. 8: Mean target gain with extrapolations

In the sparse reconstruction process ε and the number of samples selected for extrapolation provides the necessary flexibility required to find a solution which is sparse and yet agrees with the acquired data. Increasing extrapolation samples while keeping ε constant can thus offer additional degrees of freedom and contribute with further gains assuming a target stands out from noise and can be extrapolated correctly in velocity. To scrutinize this, simulations were carried out with varying number of extrapolations samples, from $E = 0$ (no extrapolation) to $E = 32$ with extrapolation of 16 samples on each side. The results of this can be seen in figure 8. It is evident that extrapolation aids sparse reconstruction in a very marked manner and can augment the coherence gain as more and more extrapolation samples are added. This can be seen at the very low SNR values where the performance is not much better than incoherent integration, but picks up rapidly as the signal level improves. Not having any extrapolation samples forces the solution to be comparable to the observed data, subject to ε, with generally low performance outcome. The other main advantage of extrapolation is that the target becomes more confined in Doppler; an example of this is given in figure 9 where compared to figure 6 the peak is now much

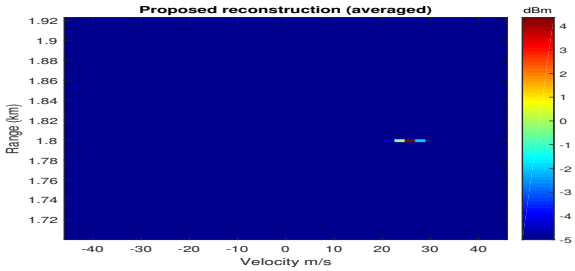

Fig. 9: Hybrid reconstruction, mean SNR = 0 dB, $E = 32$

Dette er en postprint-versjon / This is a postprint version.
DOI til publisert versjon / DOI to published version: 10.1109/RADAR.2018.8378531

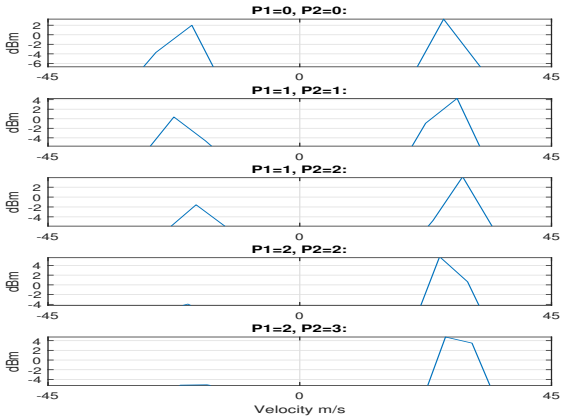

Fig. 10: Doppler profiles at target range, $E = 8$

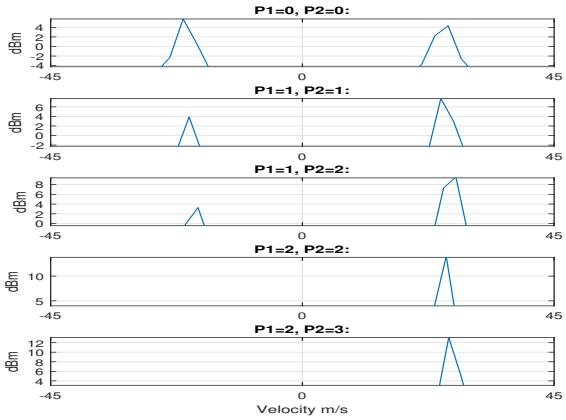

Fig. 11: Doppler profiles at target range, $E = 32$

more localized in velocity.

C. Mode A duration

It was mentioned in the previous section that the utilization of mode B alone is not sufficient to always provide unambiguous target Doppler estimates. This subsection inspects how the duration of modes A1 and A2 combined with mode B impacts the ability to resolve target velocity unambiguously. For this purpose the Doppler profiles at target range with random Swerling 1 fluctuations were averaged over 1000 independent simulations and can be seen in figure 10 under $E = 8$ extrapolations. The cases considered include $P_1 = P_2 = 0$ all the way up to $P_1 = 2, P_2 = 3$ while the number of mode B pulses $P_B = 7$ is kept fixed. Having varying number of pulses influences the Doppler bin resolution and the retrieved target gain. The simulations are therefore carried out with an average SNR of 4 dB to downplay noise relevance.

It can directly be observed from figure 10 that with mode B alone (top plot) the true velocity and the ambiguous velocity, on average, end up with the same amount of gain. In other words, the sparse reconstruction method is just as likely to position the target on an erroneous velocity as the correct one. With a high PRF and a regular sparse sampling structure this is to be expected, although the target is still likely to be detectable. Incorporating mode A1 and A2 pulses to the block benefits the arrangement as more full range pulses are made available. With two or more A1 and A2 pulses the target is generally always determined with the correct positive velocity. In figure 11 the same experiment is repeated but with an extrapolation of 16 samples on each side, where the same results are realized. The upsurge of the average peak gain is noticeable as the number of pulses gradually increases and with supplementary extrapolation samples the Doppler spread is correspondingly compact.

IV. Conclusion

Frequency diversity plays a key role in modern radar systems helping mitigate target fluctuations. Transmitting multiple waveforms with a long dwell period takes up valuable time while incoherent techniques are not capable of providing target velocity estimates or sophisticated filtering via range-Doppler maps. This article examined linking together several of these techniques incorporating frequency agility methods with coupled sparse reconstruction strategies. By transmitting a set of overlapping waveforms with doubled pulse repetition rate and performing matched-filtering with respect to several frequencies under a compressed sensing framework it was shown that full high-resolution range-Doppler maps may be generated with decisive Doppler estimates. This has the advantage of offering comparable performance using fewer pulses and a shorter time duration which was verified with considerable details through numerous simulations.

References

[1] D. Zhao and Y. Wei, "Coherent process and optimal weighting for sparse frequency agility waveform," in *IEEE Radar Conference*, 2015, pp. 334–338.

[2] W. L. Melvin and J. A. S. (Eds.), *Principles of Modern Radar*. SciTech Publishing, 2013.

[3] E. Candès, J. Romberg, and T. Tao, "Stable signal receovery from incomplete and inaccurate measurments," *Communication in Pure and Applied Mathematics*, vol. 59, pp. 1207–1223, 2006.

[4] E. J. Candès and C. Fernandez-Granda, "Towards a mathematical theory of super-resolution," *Communications on Pure and Applied Mathematics*, vol. 67, no. 6, pp. 906–956, 2014.

[5] E. Ertin, L. C. Potter, and R. L. Moses, "Sparse target recovery performance of multi-frequency chirp waveforms," in *Proc. of 19th European Signal Processing Conference (EUSIPCO)*, 2011, pp. 446–450.

[6] M. M. Hyder and K. Mahata, "Range-Doppler imaging via sparse representation," in *IEEE Radar Conference*, 2011, pp. 486–491.

[7] B. Demissie and C. R. Berger, "High-resolution range-Doppler processing by coherent block-sparse estimation," *IEEE Trans. Aerospace and Electronic Systems*, vol. 50, no. 2, April 2014.

[8] D. Cohen and Y. C. Eldar, "Reduced time-on-target in pulse Doppler radar: Slow time domain compressed sensing," in *Proc. of IEEE Radar Conference*, 2016.

[9] J. Akhtar and K. E. Olsen, "Formation of range-Doppler maps based on sparse reconstruction," *IEEE Sensors Journal*, vol. 16, no. 15, pp. 5921–5926, Aug. 2016.

[10] J. Akhtar, B. Torvik, and K. E. Olsen, "Compressed sensing with interleaving slow-time pulses and hybrid sparse image reconstruction," in *Proc. of IEEE Radar Conference*, 2017, pp. 6–10.

[11] G. Xu and Z. Xu, "Compressed sensing matrices from Fourier matrices," *IEEE Trans. Inf. Theory*, vol. 61, no. 1, pp. 469–478, Jan. 2015.

Dette er en postprint-versjon / This is a postprint version.
DOI til publisert versjon / DOI to published version: 10.1109/RADAR.2018.8378531